Virology 527 (2019) 180–187

Contents lists available at ScienceDirect

Virology

journal homepage: www.elsevier.com/locate/virology

Zika virus NS5 protein antagonizes type I interferon production via blocking TBK1 activation

Shaoli Lin[a], Shixing Yang[a,b], Jia He[a], Johnathan D. Guest[c,d], Zexu Ma[a], Liping Yang[a], Brian G. Pierce[c,d], Qiyi Tang[e], Yan-Jin Zhang[a,*]

[a] Molecular Virology Laboratory, VA-MD College of Veterinary Medicine and Maryland Pathogen Research Institute, University of Maryland, College Park, MD, USA
[b] School of Medicine, Jiangsu University, Jiangsu, China
[c] Institute for Bioscience and Biotechnology Research, University of Maryland, Rockville, MD, USA
[d] Department of Cell Biology and Molecular Genetics, University of Maryland, College Park, MD, USA
[e] Department of Microbiology, Howard University College of Medicine, Washington DC, USA

ARTICLE INFO

Keywords:
Zika virus
ZIKV
Interferon
NS5
TBK1
IRF3

ABSTRACT

Zika virus (ZIKV) is a mosquito-borne positive-sense single-stranded RNA virus in the family of *Flaviviridae*. Unlike other flaviviruses, ZIKV infection of pregnant women may result in birth defects in their newborns, such as microcephaly or vision problem. ZIKV is known to antagonize the interferon (IFN) production in infected cells. However, the exact mechanism of this interference is not fully understood. Here, we demonstrate that NS5 protein of ZIKV MR766 strain antagonizes IFN production through inhibiting the activation of TANK-binding kinase 1 (TBK1), which phosphorylates the transcription activator IFN regulatory factor 3 (IRF3). Mechanistically, NS5 interacts with the ubiquitin-like domain of TBK1 and results in less complex of TBK1 and TNF (tumor necrosis factor) receptor-associated factor 6 (TRAF6), leading to dampened TBK1 activation and IRF3 phosphorylation. Our study provides insights into the mechanism of ZIKV evasion of IFN-mediated innate immunity.

1. Introduction

Zika virus (ZIKV) was first discovered in the Zika forest in Uganda in 1947 (Hayes, 2009). The recent epidemic of ZIKV infection was reported in Brazil in 2015, and by the end of that year, the number of infected individuals was estimated to be one million in Brazil alone. The virus is also transmitted to Colombia, Puerto Rico and other 60 countries (Elliott et al., 2018; Hennessey et al., 2016; Hills et al., 2017). In the United States, ZIKV infection is also detected in the returning travelers (Hennessey et al., 2016). Based on CDC, there are 5,734 confirmed cases in the US states and 37,294 cases in the US territories as of October 16, 2018 (CDC, 2018). Many people with ZIKV infection are asymptomatic or have only mild symptoms. However, in pregnant women, ZIKV infection can cause severe microcephaly and neurological deficiency in their newborns (Britt, 2018).

ZIKV is a single-stranded, positive-sense RNA virus in the family *Flaviviridae*. Phylogenetic studies of ZIKV isolates have demonstrated that there are two distinct ZIKV lineages: Asian and African (Wang et al., 2016). Its genome is around 10 kb in length and contains a 5′ untranslated region (UTR), a single open reading frame, and a 3′ UTR (Kuno and Chang, 2007). The open reading frame encodes a single polyprotein, which is processed into the capsid (C), the precursor membrane (prM), the envelope protein (E), and seven nonstructural proteins (NS1, NS2A, NS2B, NS3, NS4A, NS4B, and NS5). Among the viral proteins, NS1, NS2A, NS2B, NS4A, NS4B, and NS5 of the Asian strains of ZIKV are reported to inhibit interferon (IFN) production (Kumar et al., 2016; Ma et al., 2018; Wu et al., 2017; Xia et al., 2018). As the largest non-structural protein of ZIKV, the NS5 protein consists of methyltransferase (MT) and RNA-dependent RNA polymerase (RdRp) domains, and between them is a short linker (Zhao et al., 2017). The MT is responsible for the 5′cap addition to viral RNA to facilitate the translation of the polyprotein (Issur et al., 2009). The RdRp is responsible for viral RNA replication and is supposed to use a de novo mechanism similar to Dengue virus (Ackermann and Padmanabhan, 2001; Kao et al., 2001; van Dijk et al., 2004).

IFN signaling is a potent host antiviral strategy during early stage viral infection. Host pattern recognition receptors (PRR) in the cytoplasm include retinoic acid-inducible gene I (RIG-I) and melanoma differentiation-associated gene 5 (MDA5) (Sato et al., 2015; Yin et al., 2017), which can recognize the viral double-stranded RNA (dsRNA).

* Corresponding author.
E-mail address: zhangyj@umd.edu (Y.-J. Zhang).

https://doi.org/10.1016/j.virol.2018.11.009
Received 17 August 2018; Received in revised form 14 November 2018; Accepted 15 November 2018
Available online 06 December 2018
0042-6822/

The PRR activation recruits the mitochondrial antiviral-signaling protein (MAVS), resulting in polymerization of the latter. The polymerized MAVS then recruits TANK-binding kinase 1 (TBK1) via TNF (tumor necrosis factor) receptor-associated factor 2, 3 and 6 (TRAF2, 3 and 6), which leads to the activation of TBK1, followed by phosphorylation and nuclear translocation of IRF3 to activate the IFN expression (Fang et al., 2017).

In ZIKV-infected cells, NS5 antagonizes host innate immune response and promotes the virus replication. In the downstream signaling of IFNs, NS5 is known to target human signal transducer and activator of transcription factor 2 (STAT2) for degradation to inhibit type I IFN induced antiviral immunity (Grant et al., 2016). In addition to STAT2 depletion, NS5 can block STAT1 phosphorylation to antagonize the IFN-activated signaling (Hertzog et al., 2018). NS5 also interacts with NOD-like-receptor-family, pyrin domain-containing 3 (NLRP3) to facilitate the formation of NLRP3-ASC-Caspase1 complex, thereby promoting the activation of inflammasome and exacerbating the inflammatory response and disease progression (Wang et al., 2018). The NS5 protein of a ZIKV strain of an Asian lineage inhibits IFN production (Kumar et al., 2016), possibly through inhibition of IRF3 according to a later study (Xia et al., 2018). However, whether NS5 of the African lineage ZIKV can inhibit IFN induction or the exact mechanism of NS5 inhibition of IFN induction is unknown. In this study, we discovered that ZIKV NS5 of MR766 strain from the African lineage antagonized the production of type I IFNs through impairing the activation of TBK1. Both MT and RdRp domains are needed for NS5 to inhibit TBK1-mediated IRF3 phosphorylation. These results provide additional insights into ZIKV interference with the IFN production.

2. Results

2.1. ZIKV NS5 inhibits polyI:C-induced IFN-β production

To determine if ZIKV MR766 strain inhibits the IFN production, we infected A549 cells with this strain at an MOI of 1. At 24 h post infection (hpi), polyI:C was transfected into the cells at 1 μg/ml. Total RNA was extracted from the cells 8 h later and subjected to RT-qPCR. The result showed that ZIKV infection reduced the polyI:C-induced IFN-β transcript to 28% in comparison with the mock-infected cells (Fig. 1A). Western blotting (WB) detection of ZIKV NS5 protein confirmed the virus proliferation in the cells. To determine if ZIKV NS5 protein contributes to this inhibitory effect, we transfected HEK293T cells with FLAG-NS5 plasmid and then stimulated the cells with polyI:C. The result showed that the cells with NS5 expression had IFN-β transcript at 22% of the cells transfected with empty vector (Fig. 1B).

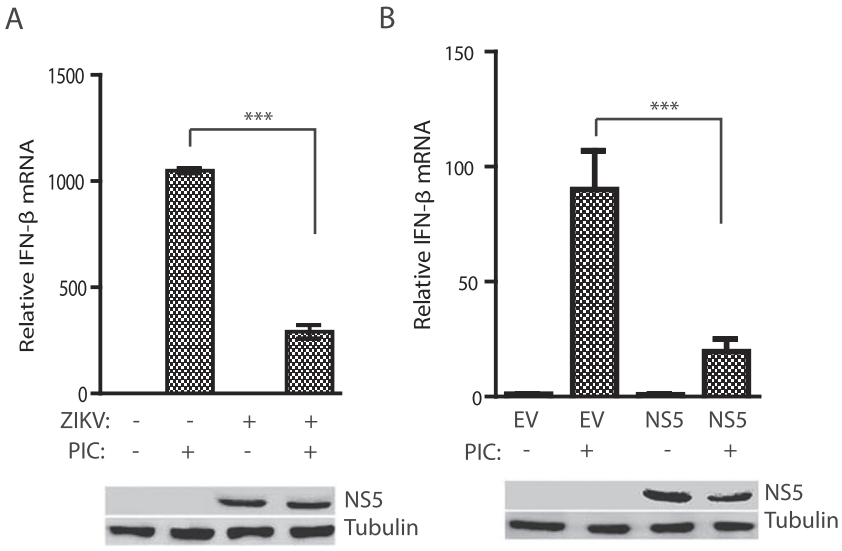

Fig. 1. ZIKV inhibits polyI:C-induced interferon expression. A. ZIKV infection of A549 cells inhibits polyI:C-induced IFN-β expression detected by RT-qPCR. The cells were infected with ZIKV MR766 strain at an MOI of 1. At 24 h post infection (hpi), the cells were transfected with polyI:C (PIC). The cells were harvested 8 h post polyI:C treatment for RNA isolation and qPCR. Significant difference between mock-infected and MR766-infected cells post polyI:C is denoted with *** for $P < 0.001$. Western blotting images of NS5 and tubulin are shown below the graph. B. ZIKV NS5 inhibits IFN induction in HEK293T cells. The cells were transfected with NS5 plasmid and, 24 h later, stimulated with polyI:C. EV; empty vector.

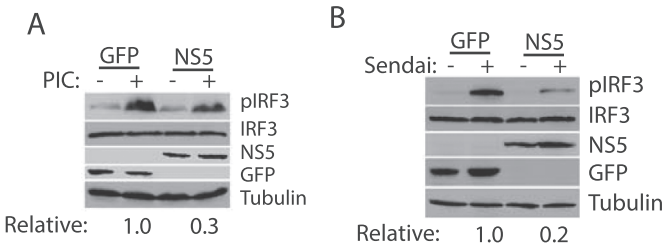

Fig. 2. ZIKV NS5 inhibits IRF3 phosphorylation. A. NS5 inhibits polyI:C-induced phosphorylation of IRF3 in 293-IRF3 cells. The 293-IRF3 cells were transfected with GFP and NS5 plasmids and, 24 h later, transfected with polyI:C (PIC). Western blotting of phosphor-IRF3 (pIRF3) and total IRF3 was conducted. Relative levels of pIRF3 after PIC stimulation are shown below the images. B. NS5 inhibits Sendai virus-induced IRF3 phosphorylation in 293-IRF3 cells. The 293-IRF3 cells were transfected with GFP and NS5 plasmids. At 24 h post transfection, the cells were infected with Sendai virus. The cells were harvested for Western blotting 15 hpi.

2.2. ZIKV NS5 inhibits the phosphorylation of IRF3

To determine the mechanism of NS5 inhibition of IFN induction, we established HEK293 cells stably expressing IRF3 (293-IRF3). We transfected 293-IRF3 cells with NS5-expressing plasmid and tested its effect on IRF3 activation as IRF3 is a critical transcription activator in IFN induction (Collins et al., 2004). The cells were transfected with polyI:C the next day and harvested for WB. The result showed that NS5 reduced the level of phosphorylated IRF3 (pIRF3) by 70% in comparison with the empty vector control, whereas the total IRF3 protein level had minimal change (Fig. 2A). As polyI:C is a synthetic analog of dsRNA and may not mimic natural virus infection, we verified the observation of an NS5-induced reduction of pIRF3 with Sendai virus infection. After NS5 transfection for 24 h, 293-IRF3 cells were infected with Sendai virus at an MOI of 1. The infected cells were harvested for Western blot analysis at 15 h post infection (hpi). The result showed that NS5 attenuated Sendai virus-induced pIRF3 by 80% compared to the GFP control (Fig. 2B). These results indicate that NS5 blocks IRF3 activation.

2.3. NS5 inhibits TBK1-induced activation of IRF3 and both MT and RdRp domains are needed

The IFN induction pathway can be activated by the overexpression of individual upstream components (Nan et al., 2014), such as TBK1

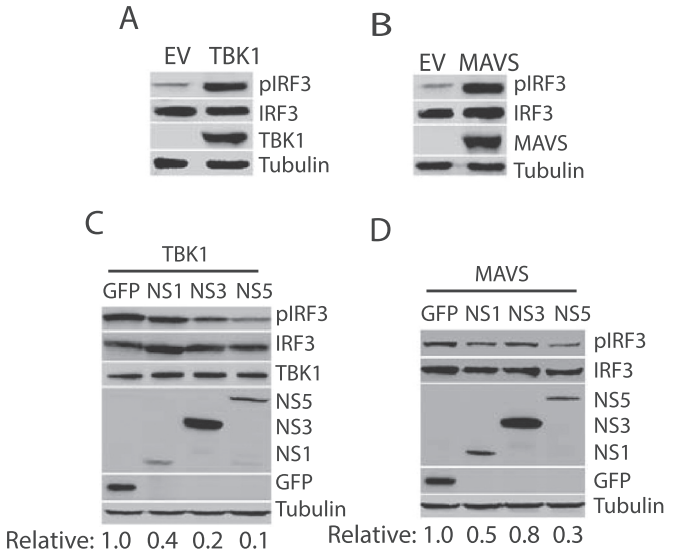

Fig. 3. NS5 inhibits TBK1-induced IRF3 activation. A. TBK1 induces IRF3 activation in 293-IRF3 cells. The 293-IRF3 cells were harvested 48 h after transfection for WB. B. MAVS activates IRF3. C. NS5 inhibits TBK1-induced IRF3 activation in 293-IRF3 cells. Relative levels of pIRF3 after normalization with IRF3 are shown below the images. D. NS5 inhibits MAVS-induced IRF3 activation in 293-IRF3 cells.

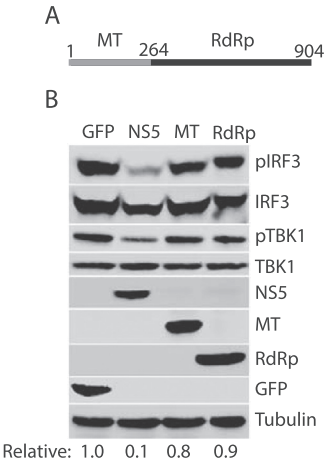

Fig. 4. Both methyltransferase (MT) and RNA-dependent RNA polymerase (RdRp) domains of NS5 are needed for the inhibition of IRF3 activation. A. Schematic illustration of MT and RdRp domain positions in NS5. The numbers above the line denote amino acid positions in NS5 protein. B. WB detection of the effect of MT and RdRp on IRF3 activation. The 293-IRF3 cells were co-transfected with HA-TBK1 and one of the following plasmids: GFP, FLAG-NS5, FLAG-MT, and FLAG-RdRp. WB with antibodies against pIRF3, IRF3, pTBK1, TBK1, FLAG and GAPDH was done. Relative levels of pIRF3 after normalization with IRF3 are shown below the images.

and MAVS (Fig. 3A&B). To identify the step that NS5 targets to inhibit the IFN signaling, we transfected 293-IRF3 cells with the plasmids of NS5 and MAVS, or NS5 and TBK1. ZIKV NS1 and NS3 were included in the co-transfection as controls as NS1 was reported to inhibit IFN induction (Wu et al., 2017). The results showed that NS5 reduced the pIRF3 level in both co-transfections with TBK1 and MAVS (Figs. 3C&D). Both NS1 and NS3 reduced TBK1-induced pIRF3, whereas NS1 also reduced MAVS-induced pIRF3 (Figs. 3C&D). Because we focused on the NS5 effect on IFN induction, we did not pursue further work for NS1 and NS3. Since TBK1 phosphorylates IRF3 upon activation, we speculated that NS5 could target TBK1 or its downstream steps for impairment of IFN induction.

NS5 consists of MT and RdRp domains (Zhao et al., 2017). To identify whether any one of the two domains of NS5 plays a role in the inhibition of pIRF3, we cloned the NS5 sequences for MT and RdRp for transient expression (Fig. 4A). The 293-IRF3 cells were transfected with the plasmids of MT and TBK1, or RdRp and TBK1. The Western blotting result showed that only the full-length NS5 could attenuate the pIRF3, whereas the MT or RdRp domain alone had minimal effect on the pIRF3 level (Fig. 4B). Also, the level of phosphorylated TBK1 (pTBK1) also decreased in the presence of full-length NS5 but not MT or RdRp (Fig. 4B). These results indicate that full-length NS5 impairs the activation of TBK1 and both MT and RdRp domains are needed for this inhibitory effect.

2.4. ZIKV NS5 interacts with TBK1

To further explore the mechanism that NS5 inhibits IFN signaling and test if NS5 interacts with TBK1, co-immunoprecipitation (co-IP) was performed. Co-IP of NS5 precipitated TBK1 but not GFP (Fig. 5A). Similarly, co-IP of TBK1 precipitated NS5 but not GFP (Fig. 5B). Immunoblotting of whole cell lysate confirmed the expression of the individual proteins. The result indicates that NS5 possibly inhibits IFN induction through interaction with TBK1.

2.5. The NS5 interaction with TBK1 leads to lower TBK1 in complex with TRAF6

In the resting state, TBK1 pre-associates with TRAF2, 3 and 6 in the

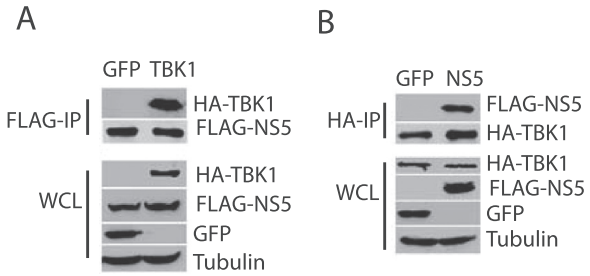

Fig. 5. NS5 interacts with TBK1 detected by co-immunoprecipitation (co-IP). A. FLAG IP of NS5 co-precipitates TBK1 but not GFP. HEK293T cells were transfected with HA-TBK1 and FLAG-NS5 plasmids. GFP plasmid was included as a control. WB of whole cell lysate (WCL) was also done. B. HA IP of TBK1 co-precipitates NS5 but not GFP.

cells (Fang et al., 2017). Upon the activation of the RLR pathway, polymerized MAVS recruits TRAFs and subsequently activates TBK1. To determine the reason for the attenuated activation of TBK1 by NS5, we transfected HEK293T cells with the plasmids of TBK1, TRAF6, and NS5 for co-IP. Result showed that co-IP of TBK1 precipitated less TRAF6 in the presence of NS5 than the GFP control (Fig. 6A). Also, co-IP of TRAF6 precipitated less TBK1 in the presence of NS5 than the GFP control (Fig. 6B), which demonstrates that the NS5 interaction with TBK1 leads to less TBK1 in complex with TRAF6.

To exclude the possibility that NS5 binds to TRAF6 to disrupt the interaction between TRAF6 and TBK1, we conducted co-IP from lysate of cells transfected with NS5 and TRAF6 without TBK1. The result showed that the IP of TRAF6 did not yield detectable level NS5 (Fig. 6C), which suggests that there is possibly no direct interaction between TRAF6 and NS5 (Fig. 6C). Overall, these results indicate that NS5 binds to TBK1 and may consequently interferes with its downstream signaling of IFN induction.

2.6. The ULD domain of TBK1 is required for interaction with NS5

To map the domain of TBK1 in its interaction with NS5, we constructed truncated TBK1 clones (Fig. 7A). There are four domains in TBK1, namely kinase domain (KD), ubiquitin-like domain (ULD),

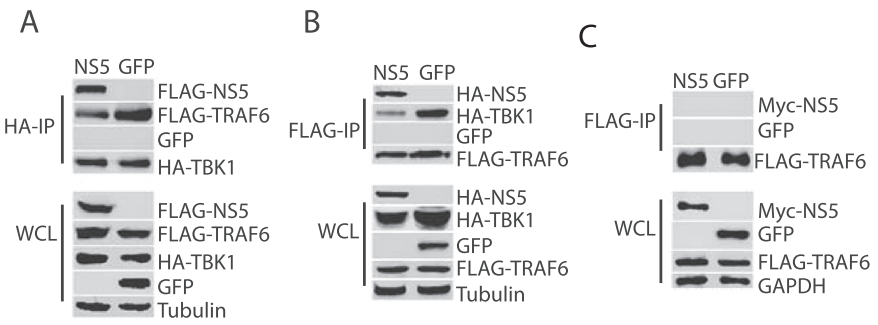

Fig. 6. NS5 interaction with TBK1 leads to lower TBK1 in complex with TRAF6. A. HA IP of TBK1 co-precipitates less TRAF6 in the presence of NS5 than GFP. HEK293T cells were co-transfected with FLAG-NS5, HA-TBK1 and FLAG-TRAF6. At 36 hpt, the cells were lysed and subjected to co-IP for TBK1, followed by WB for NS5 and TRAF6. B. FLAG IP of TRAF6 co-precipitates less TBK1 in the presence of NS5 than GFP. C. FLAG IP of TRAF6 fails to co-precipitate NS5 in the absence of TBK1 co-transfection. HEK293T cells were transfected with TRAF6 and NS5. IP for TRAF6, followed by WB for NS5, was done.

scaffold dimerization domain (SDD) and c-terminal domain (CD) (Larabi et al., 2013; Xiang et al., 2016). Truncation clone TBK1-D1 contained only KD; TBK1-D2 consisted of KD and ULD; and TBK1-D3 was composed of KD, ULD, and SDD.

HEK293T cells were transfected with NS5 and TBK1 or the truncated TBK1 clones. Co-IP of NS5 was done, followed by Western blotting to determine the presence of full length or the truncated TBK1 in the precipitates. The result showed that co-IP of NS5 precipitated TBK1, TBK1-D2, and TBK1-D3, but not TBK1-D1 (Fig. 7B), which suggests that the ULD of TBK1 is required for the interaction of TBK1 with NS5.

To locate the possible interaction sites between TBK1 and ZIKV NS5, we used structural data of TBK1 and NS5 to perform computational docking and predict a TBK1-NS5 complex structure (Fig. 7C). Initial models of the TBK1 homodimer and NS5 monomer closely matched existing crystal structures of both proteins (Larabi et al., 2013; Zhao et al., 2017). The modeled complex suggests that NS5 may bind to TBK1 with its “groove” formed in the linker section between MT and RdRp domains (Fig. 7D). Detailed inspection of the modeled complex found some residue pairs across the interface that may contribute to complex formation, such as S347 in the ULD (Fig. 7E). To validate the importance of this residue in the TBK1 interaction with NS5, we conducted mutagenesis of TBK1-D2 and generated FLAG-TBK1-D2m (S347A). Co-transfection and co-IP were done to determine if the S347A mutation in TBK1 ULD compromised the TBK1 interaction with NS5. The result showed that both the wild-type and mutant TBK1-D2 co-precipitated ZIKV NS5 to a similar extent (Fig. 7F), which indicates that the S347A mutation does not detectably disrupt the complex formation.

3. Discussion

Our study elucidates the mechanism of ZIKV NS5 protein in the inhibition of IFN induction. NS5 interacts with TBK1 to inhibit the IRF3 phosphorylation and the consequent IFN expression. Both the MT and RdRp domains are needed in the inhibition of IRF3 activation. The ULD of TBK1 is required for the TBK1 interaction with NS5. This further provides insight into the roles of NS5 in antagonizing the innate immunity. ZIKV NS5 is a vital viral protein that is responsible for viral RNA replication and antagonizing of cellular innate immune response.

TBK1 is an important host regulator in several cellular processes or signaling pathways, such as autophagy, cell mitosis, apoptosis and immune response (Cruz and Brekken, 2018; Delhase et al., 2012). Some cancers and virus infections are associated with the abnormal TBK1 activity (Cruz and Brekken, 2018). During their invasion of the host, some viruses are known to interfere with the physiological function of TBK1. For instance, hepatitis E virus inhibits TBK1 activation via its non-structural protein PCP (Nan et al., 2014). ZIKV and HCMV both induce mitochondrial re-localization of pTBK1 and mitosis in ZIKV-infected NES (neuroepithelial stem) cells, and the inhibition of TBK1 activity can increase the apoptosis of ZIKV-infected NCX (neocortical)-NES cells (Onorati et al., 2016).

There are two lineages of ZIKV strains, the Asian and African lineages (CDC, 2018). The comparison between strains from the two lineages showed that the African MR766 strain causes more severe brain damage and postnatal fatality than the Asian MEX1–44 strain (Shao et al., 2017). In the process of innate immunity evasion, the non-structural proteins of ZIKV are notorious for their inhibition of IFN induction and its downstream singling. Among the non-structural proteins, NS2B3 of MR766 strain is demonstrated to dampen the IFN pathway by cleaving human STING while the NS2B3 of the Asian strain (Z1106033) is demonstrated to inhibit IFN-activated signaling by degrading JAK1 (Ding et al., 2018; Wu et al., 2017). A recent study showed that NS2A, NS2B, and NS4B of the Asian FSS13025 strain are all able to block the IFN production via inhibition of TBK1 activity, while NS5 targets downstream of IRF3 through binding with IRF3 (Xia et al., 2018). Moreover, one single amino acid mutation (A188V) of the NS1 protein of FSS13025 renders the protein to gain the ability to inhibit IFN induction (Xia et al., 2018). NS4A of an Asian strain is also reported to impair IFN signaling by binding to MAVS and block the interaction between MAVS and RIG-I (Ma et al., 2018). In our study, we could not detect the interaction between MR766 NS5 protein and IRF3 upon IFN induction by exogenous RIG-I (data not shown). Sequence alignment of the NS5 proteins from MR766 and the two strains of Asian lineage, FSS13025, and PRABC-59, showed that there are dozens of amino acid variations, which may lead to different amino acids arrangement and protein binding preference of the NS5 proteins.

It is notable that neither MT nor RdRp domain alone of MR766 NS5 exerts inhibition of IFN induction, suggesting that the overall conformational structure of NS5 is essential for its interaction with TBK1. The analysis of the overall structure of TBK1 dimer in complex with NS5 indicates that the “groove” formed by MT and RdRp domains interacts with the ULD domain of TBK1. The presence of NS5 leads to lower TBK1 in complex with TRAF6 than GFP control, which is demonstrated by co-IP. Further co-IP showed that NS5 has no detectable direct interaction with TRAF6, suggesting that NS5 interaction with TBK1 might make it less available in complex with TRAF6. The ULD of TBK1 is required for TBK1 interaction with NS5. The ULD spanning from amino acid (aa) residues 300–382 of TBK1 is located between KD and SDD domains (Fig. 7A). One of the functions of ULD is to mediate protein-protein interaction in signal transduction (Welchman et al., 2005), while the TBK1 homodimer is not mediated by ULD alone (Li et al., 2012). ULD binds to KD and SDD and the interaction among the domains helps to stabilize the TBK1 dimer (Tu et al., 2013). The deletion of ULD leads to the loss of kinase activity of TBK1; and mutations of L352A/I353A in ULD blocks TBK1-induced IFN-β production (May et al., 2004). The mutations of E355A, R357A, and E355A/R357A in the dimeric interface also impaired the TBK1 phosphorylation (Li et al., 2012), suggesting that ULD is indispensable for the TBK1 function. TRAF proteins are known to interact with TBK1 through SDD (Fang et al., 2017). Since ULD is adjacent to SDD, the interaction of ZIKV NS5 to ULD could block the binding site of TRAF6 on SDD, which might affect the access of TRAF6 to TBK1.

Our model of TBK1 and NS5 interaction suggests that S347 residue in the ULD might contribute to the complex formation. However, S347A mutation does not affect TBK1 interaction with NS5. This could be the result of local inaccuracies in the model and further refinement is needed. There might be compensatory interface effects from alanine

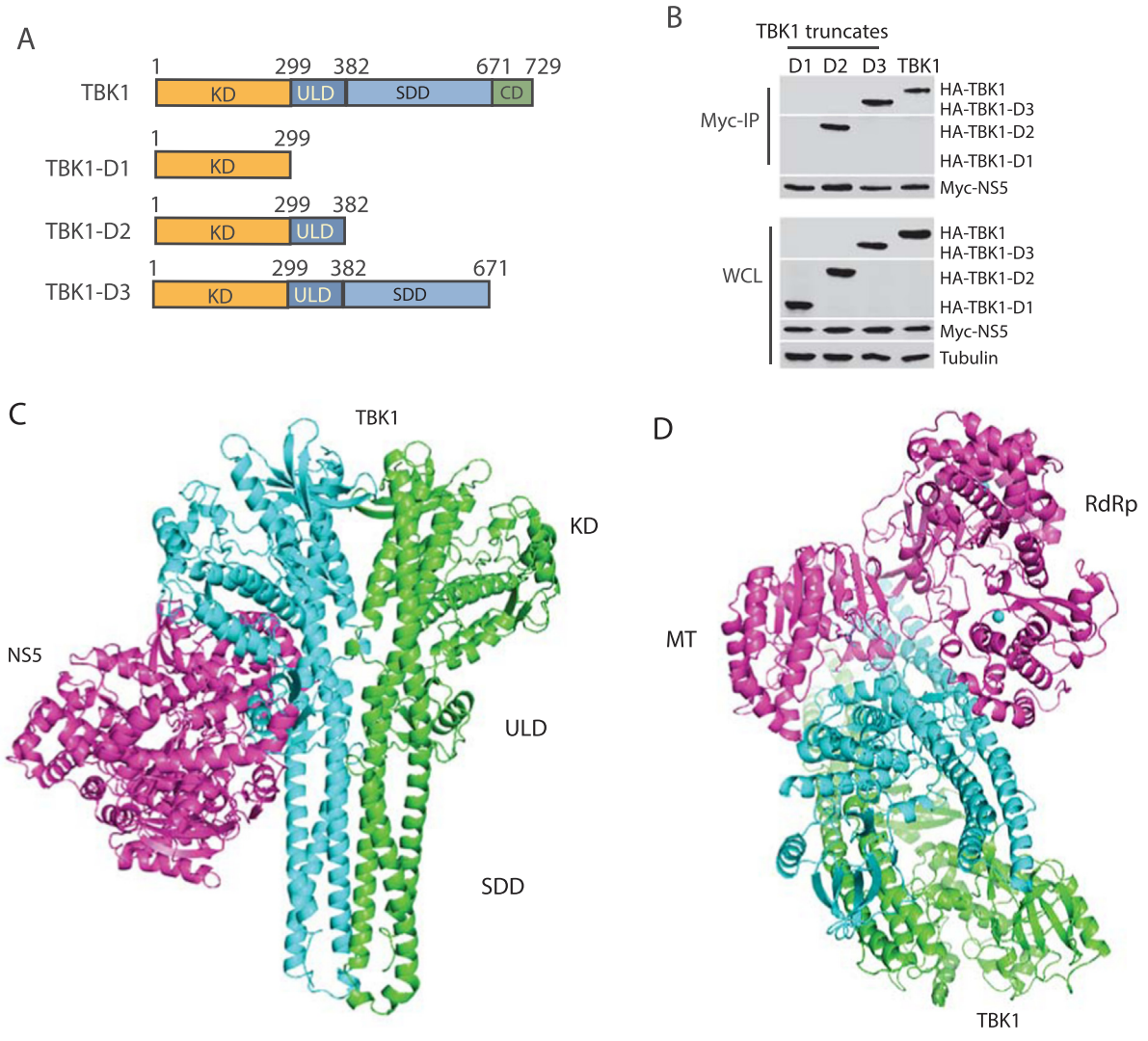

(caption on next page)

Fig. 7. The ULD domain of TBK1 is required for interaction with NS5. A. Schematic illustration of TBK1 domain positions. KD: kinase domain; ULD: ubiquitin-like domain; SDD: scaffold dimerization domain; CD: C-terminal domain. The numbers denote amino acid positions in TBK1 protein. B. Myc IP of NS5 co-precipitates TBK1, TBK1-D2, and TBK1-D3 but not TBK1-D1. WB of whole cell lysate (WCL) was also done. C. Overall structure of the TBK1 dimer in complex with NS5. The first unit of TBK1 is colored as blue, the second unit of TBK1 is colored as green, and the NS5 is colored as magenta. The domains of TBK1 in the dimer are labeled as KD, ULD, SDD and CTD. D. Top view of TBK1 in complex with NS5. The colors are indicated as panel C. The MT and RdRp domains are noted. E. Predicted interface of TBK1 and NS5 is shown, with possible key residues involved in hydrogen bonding and hydrophobic contacts found in SDD and ULD highlighted as sticks. Two residues in TBK1, S347 and E617, were predicted to be involved in hydrogen bonds with NS5, with the specific interactions indicated by black dotted lines between residues. Three other residues were predicted to be involved in hydrophobic interactions with NS5. F. The S347A mutation in TBK1 does not affect TBK1 interaction with NS5 detected by co-IP. HEK293T cells were co-transfected with the FLAG-TBK1-D2m and Myc-NS5. Wild-type TBK1-D2 was included as a control.

substitution that mitigate the effect of the putative hydrogen bond loss, such as bound interface water molecules or local side chain re-arrangements. Future mutagenesis of other predicted interface residues may lead to the identification of the key residues in the binding.

Collectively, our study demonstrates that the NS5 protein of ZIKV MR766 strain inhibits the IFN induction by interacting with TBK1, leading to the reduction of TBK1 activation and consequently lower IFN expression. The ULD of TBK1 is required for the interaction of TBK1 with NS5, while both MT and RdRp domains of NS5 are needed for the binding. This finding provides further insights into the ZIKV interference with the host innate immunity.

4. Materials and methods

4.1. Cells and viruses

A549 (ATCC® CCL-185™), HEK293, and HEK293T were maintained in DMEM medium supplemented with 10% fetal bovine serum (FBS). HEK293 cell stably expressing IRF3 (293-IRF3 cells) was established previously (Nan et al., 2014). The ZIKV MR766 strain (ATCC VR-84) and Sendai virus (ATCC VR-907) were obtained from the ATCC.

4.2. Plasmids

ZIKV NS5, MT and RdRp domains were amplified with PCR from ZIKV MR766 strain (GenBank Accession Number: AY632535.2) and then cloned into the vector pCAGEN (Addgene plasmid number 11160) with FLAG, hemagglutinin (HA) or Myc tag at the N terminus. Human TBK1 was amplified and then cloned to pCAGEN with an HA or FLAG tag at the N terminus. TBK1 truncations were constructed into pCAGEN-HA or FLAG vector. TBK1 S347Amutation was constructed into pCAGEN-FLAG vector. All primers used for plasmid construction are listed in Table 1. All in-house-constructed plasmids were subjected to DNA sequencing. The construction of Myc-RIG-I (N-terminal domain) and Myc-MAVS (Nan et al., 2014) were described previously.

4.3. Transfection

Transfection of HEK293T and 293-IRF3 cells with plasmid DNA was performed by using FuGene HD transfection reagent (Promega, Madison, WI) according to the instructions of the manufacturer. Poly I:C (low molecular weight), a synthetic analog of dsRNA (Invivogen, San Diego, CA), was used to induce interferon production at the final concentration of 1 μg/ml.

4.4. Western blot analysis

Cells were lysed in Laemmli sample buffer, followed by sodium dodecyl sulfate-polyacrylamide gel electrophoresis (SDS-PAGE) and Western blotting as previously described (Yang et al., 2018). Antibodies against green fluorescence protein (GFP) (Santa Cruz Biotechnology, Inc., Dallas, TX), IRF3 (Santa Cruz), phospho-IRF3 (Ser396) (Cell Signaling Technology, Danvers, MA), HA (Thermo Fisher Scientific, Waltham, MA), Myc (Thermo Fisher), FLAG (Sigma-Aldrich, St. Louis, MO), GAPDH (Santa Cruz), TBK1 (Santa Cruz), phospho-TBK1 (Ser172) (Cell Signaling), β-tubulin (Sigma-Aldrich), ZIKV NS1, NS3, and NS5 (GeneTex, Inc., Irvine, CA) were used in the blotting. The chemiluminescence signal was collected with the Quantity One Program, version 4.6 and a ChemiDoc XRS imaging system (Bio-Rad Laboratories, Hercules, CA).

4.5. Reverse transcription and real-time quantitative PCR (RT-qPCR)

Total RNA was isolated from A549 or HEK293T cells with TRIzol reagent (Thermo Fisher). Reverse transcription was done with avian myeloblastosis virus (AMV) reverse transcriptase, oligo (dT) and a random 15-mer oligo. Real-time PCR of IFN-β and RPL32 (ribosomal protein L32, as an internal control) transcripts was performed with SYBR green Supermix (Thermo Fisher) as described (Nan et al., 2012).

4.6. Co-Immunoprecipitation (Co-IP)

IP was conducted as previously described with modifications (Nan et al., 2014). Briefly, HEK293T cells were lysed with lysis buffer

Table 1
List of primers used in this study.

Primer[a]	Sequences (5′ to 3′)[b]	Target gene
MT-F	T*GAATTC* GGAGGTGGGACGGGAGAG	NS5 MT
MT-R	T*CTCGAG*TCACTTTGCCCCAGAGACCCAGTA	
RdRp-F	C*GAATTC* AGCAACATCATAAAAAGTGTG	NS5 RdRp
RdRp-R	T*CTCGAG*TTACAACACTCCGGGTGTGGAC	
TBK1-F	AACGTCT*CGAATTCC*AGAGCACTTCTAATCATCTG	TBK1
TBK1-R	C*CTCGAG*CTAAAGACAGTCAACGTTGCGAAG	
TBK1-D1-R	CG*CTCGAG*TTAAAAAAACTGGTCAAAACCCCAAC	TBK1-D1
TBK1-D2-R	A*CTCGAG*TTATACTACAAATATAGGGTTTTC	TBK1-D2
TBK1-D3-R	G*CTCGAG*TTAATGTTTGATTCCACTGGAAGCTG	TBK1-D3
TBK1 mULD-F1	CCAAAATTATTTCTGCAAATCAAGAACTTATCTACGAAGG	TBK1-D2m
TBK1 mULD-R1	TAAGTTCTTGATTTGCAGAAATAATTTTGGTTTGTTTATA	TBK1-D2m

[a] F: forward primer, R: reverse primer. The NS5 primers are based on sequences of ZIKV MR766 (GenBank accession number AY632535).
[b] The italicized letters indicate restriction enzyme cleavage sites for cloning.

(50 mM Tris, pH7.4, 150 mM NaCl, 0.2 mM EDTA, 2 mM EGTA, 0.5% IGEPAL CA-630, 10% glycerol, 1 mM sodium vanadate). The lysate was subjected to centrifugation at 14,000 ×*g* for 5 min at 4 °C. Antibodies against HA, Myc or FLAG were added to the supernatant. IP with protein A/G agarose (KPL Inc., Gaithersburg, MD) was done according to the manufacturer's instructions. The IP samples were subjected to immunoblot analysis with antibodies against the individual proteins indicated in results.

4.7. Statistical analysis

The difference in the IFN-β mRNA level between the group in the presence of ZIKV replication and the mock-infected control sample was assessed by the Student *t*-test. A two-tailed P value of less than 0.05 was considered significant.

4.8. Predictive docking and modeling

Individual models of the TBK1 homodimer and NS5 were generated by SWISS-MODEL (Waterhouse et al., 2018) from the full-length FASTA sequences of both proteins. The models were docked using ZDOCK (Pierce et al., 2014) with all residues in TBK1 except for those in ULD blocked from forming part of the complex interface. A top prediction from the ZDOCK output was then refined in protein modeling software Rosetta, version 3 (weekly release 2018.12), using a high-resolution docking protocol (Gray et al., 2003) to generate 1200 locally refined models, followed by rescoring in ZRANK (Pierce and Weng, 2008) to select a refined model. Assessment of hydrogen bonds in the predicted interface was performed using HBPLUS software (McDonald and Thornton, 1994). Visualization of models was performed using PyMOL software (pymol.org).

Acknowledgment

S. Lin was partially sponsored by Chinese Scholarship Council. This study was partially funded by a seed grant from the University of Maryland, College Park, MD. J. Guest was supported by NIH T32 AI125186 (Virology Training Grant).

Competing financial interests

The authors declare no competing financial interests.

Author Contribution

S.L.: 1, 2, 3, 13 and 14. S.Y.: 1, 2, 3, and14. J.H.: 2 and 14. J.G.: 6 and 14. Z.M.: 2 and 14. Q.T.: 8 and 14. L.Y.: 2 and 14. B.P.: 6, 9, and 14. Y.Z.: 1, 2, 3, 4, 5, 6, 7, 8, 10, 13 and 14.

References

Ackermann, M., Padmanabhan, R., 2001. De novo synthesis of RNA by the dengue virus RNA-dependent RNA polymerase exhibits temperature dependence at the initiation but not elongation phase. J. Biol. Chem. 276, 39926–39937.

Britt, W.J., 2018. Adverse outcomes of pregnancy-associated Zika virus infection. Semin. Perinatol.

CDC, 2018. Zika Cases in the United States. 〈https://www.cdc.gov/zika/reporting/case-counts.html〉.

Collins, S.E., Noyce, R.S., Mossman, K.L., 2004. Innate cellular response to virus particle entry requires IRF3 but not virus replication. J. Virol. 78, 1706–1717.

Cruz, V.H., Brekken, R.A., 2018. Assessment of TANK-binding kinase 1 as a therapeutic target in cancer. J. Cell Commun. Signal. 12, 83–90.

Delhase, M., Kim, S.-Y., Lee, H., Naiki-Ito, A., Chen, Y., Ahn, E.-R., Murata, K., Kim, S.-J., Lautsch, N., Kobayashi, K.S., Shirai, T., Karin, M., Nakanishi, M., 2012. TANK-binding kinase 1 (TBK1) controls cell survival through PAI-2/serpinB2 and transglutaminase 2. Proc. Natl. Acad. Sci. USA 109, E177–E186.

Ding, Q., Gaska, J.M., Douam, F., Wei, L., Kim, D., Balev, M., Heller, B., Ploss, A., 2018. Species-specific disruption of STING-dependent antiviral cellular defenses by the Zika virus NS2B3 protease. Proc. Natl. Acad. Sci. USA.

Elliott, R., Banerjee, T., Santra, S., 2018. Zika: an emerging disease requiring prevention and awareness. PLoS Negl. Trop. Dis. 12, e0006486.

Fang, R., Jiang, Q., Zhou, X., Wang, C., Guan, Y., Tao, J., Xi, J., Feng, J.-M., Jiang, Z., 2017. MAVS activates TBK1 and IKKε through TRAFs in NEMO dependent and independent manner. PLoS Pathog. 13, e1006720.

Grant, A., Ponia, S.S., Tripathi, S., Balasubramaniam, V., Miorin, L., Sourisseau, M., Schwarz, M.C., Sanchez-Seco, M.P., Evans, M.J., Best, S.M., Garcia-Sastre, A., 2016. Zika virus targets human STAT2 to inhibit type I interferon signaling. Cell Host Microbe 19, 882–890.

Hayes, E.B., 2009. Zika virus outside Africa. Emerg. Infect. Dis. 15, 1347–1350.

Hennessey, M., Fischer, M., Staples, J.E., 2016. Zika virus spreads to new areas - region of the Americas, May 2015-January 2016. Morb. Mortal. Wkly Rep. 65, 55–58.

Hertzog, J., 2018. Dias Junior, A.G., Rigby, R.E., Donald, C.L., Mayer, A., Sezgin, E., Song, C., Jin, B., Hublitz, P., Eggeling, C., Kohl, A., Rehwinkel, J. Infection with a Brazilian isolate of Zika virus generates RIG-I stimulatory RNA and the viral NS5 protein blocks type I IFN induction and signaling. Eur J Immunol.

Hills, S.L., Fischer, M., Petersen, L.R., 2017. Epidemiology of Zika Virus Infection. J. Infect. Dis. 216, S868–s874.

Issur, M., Geiss, B.J., Bougie, I., Picard-Jean, F., Despins, S., Mayette, J., Hobdey, S.E., Bisaillon, M., 2009. The flavivirus NS5 protein is a true RNA guanylyltransferase that catalyzes a two-step reaction to form the RNA cap structure. RNA 15, 2340-2350.

Kao, C.C., Singh, P., Ecker, D.J., 2001. De novo initiation of viral RNA-dependent RNA synthesis. Virology 287, 251–260.

Kumar, A., Hou, S., Airo, A.M., Limonta, D., Mancinelli, V., Branton, W., Power, C., Hobman, T.C., 2016. Zika virus inhibits type-I interferon production and downstream signaling. EMBO Rep. 17, 1766–1775.

Kuno, G., Chang, G.J., 2007. Full-length sequencing and genomic characterization of Bagaza, Kedougou, and Zika viruses. Arch. Virol. 152, 687–696.

Larabi, A., Devos, J.M., Ng, S.L., Nanao, M.H., Round, A., Maniatis, T., Panne, D., 2013. Crystal structure and mechanism of activation of TANK-binding kinase 1. Cell Rep. 3, 734–746.

Li, J., Li, J., Miyahira, A., Sun, J., Liu, Y., Cheng, G., Liang, H., 2012. Crystal structure of the ubiquitin-like domain of human TBK1. Protein Cell 3, 383–391.

Ma, J., Ketkar, H., Geng, T., Lo, E., Wang, L., Xi, J., Sun, Q., Zhu, Z., Cui, Y., Yang, L., Wang, P., 2018. Zika virus non-structural protein 4A blocks the RLR-MAVS signaling. Front. Microbiol. 9.

May, M.J., Larsen, S.E., Shim, J.H., Madge, L.A., Ghosh, S., 2004. A novel ubiquitin-like domain in IkappaB kinase beta is required for functional activity of the kinase. J. Biol. Chem. 279, 45528–45539.

Nan, Y., Wang, R., Shen, M., Faaberg, K.S., Samal, S.K., Zhang, Y.J., 2012. Induction of type I interferons by a novel porcine reproductive and respiratory syndrome virus isolate. Virology 432, 261–270.

Nan, Y., Yu, Y., Ma, Z., Khattar, S.K., Fredericksen, B., Zhang, Y.J., 2014. Hepatitis E virus inhibits type I interferon induction by ORF1 products. J. Virol. 88, 11924–11932.

Onorati, M., Li, Z., Liu, F., Sousa, A.M.M., Nakagawa, N., Li, M., Dell'Anno, M.T., Gulden, F.O., Pochareddy, S., Tebbenkamp, A.T.N., Han, W., Pletikos, M., Gao, T., Zhu, Y., Bichsel, C., Varela, L., Szigeti-Buck, K., Lisgo, S., Zhang, Y., Testen, A., Gao, X.B., Mlakar, J., Popovic, M., Flamand, M., Strittmatter, S.M., Kaczmarek, L.K., Anton, E.S., Horvath, T.L., Lindenbach, B.D., Sestan, N., 2016. Zika virus disrupts phospho-TBK1 localization and mitosis in human neuroepithelial stem cells and radial glia. Cell Rep. 16, 2576–2592.

Pierce, B., Weng, Z., 2008. A combination of rescoring and refinement significantly improves protein docking performance. Proteins 72, 270–279.

Sato, S., Li, K., Kameyama, T., Hayashi, T., Ishida, Y., Murakami, S., Watanabe, T., Iijima, S., Sakurai, Y., Watashi, K., Tsutsumi, S., Sato, Y., Akita, H., Wakita, T., Rice, C.M., Harashima, H., Kohara, M., Tanaka, Y., Takaoka, A., 2015. The RNA sensor RIG-I dually functions as an innate sensor and direct antiviral factor for hepatitis B virus. Immunity 42, 123–132.

Shao, Q., Herrlinger, S., Zhu, Y.N., Yang, M., Goodfellow, F., Stice, S.L., Qi, X.P., Brindley, M.A., Chen, J.F., 2017. The African Zika virus MR-766 is more virulent and causes more severe brain damage than current Asian lineage and dengue virus. Development 144, 4114–4124.

Tu, D., Zhu, Z., Zhou, A.Y., Yun, C.-H., Lee, K.-E., Toms, A.V., Li, Y., Dunn, G.P., Chan, E., Thai, T., Yang, S., Ficarro, S.B., Marto, J.A., Jeon, H., Hahn, W.C., Barbie, D.A., Eck, M.J., 2013. Structure and ubiquitination-dependent activation of tank-binding kinase 1. Cell Rep. 3. https://doi.org/10.1016/j.celrep.2013.1001.1033.

van Dijk, A.A., Makeyev, E.V., Bamford, D.H., 2004. Initiation of viral RNA-dependent RNA polymerization. J. Gen. Virol. 85, 1077–1093.

Wang, L., Valderramos, S.G., Wu, A., Ouyang, S., Li, C., Brasil, P., Bonaldo, M., Coates, T., Nielsen-Saines, K., Jiang, T., Aliyari, R., Cheng, G., 2016. From mosquitos to humans: genetic evolution of zika virus. Cell Host Microbe 19, 561–565.

Wang, W., Li, G., De, W., Luo, Z., Pan, P., Tian, M., Wang, Y., Xiao, F., Li, A., Wu, K., Liu, X., Rao, L., Liu, F., Liu, Y., Wu, J., 2018. Zika virus infection induces host inflammatory responses by facilitating NLRP3 inflammasome assembly and interleukin-1beta secretion. Nat. Commun. 9, 106.

Welchman, R.L., Gordon, C., Mayer, R.J., 2005. Ubiquitin and ubiquitin-like proteins as multifunctional signals. Nat. Rev. Mol. Cell Biol. 6, 599–609.

Wu, Y., Liu, Q., Zhou, J., Xie, W., Chen, C., Wang, Z., Yang, H., Cui, J., 2017. Zika virus evades interferon-mediated antiviral response through the co-operation of multiple nonstructural proteins in vitro. Cell Discov. 3, 17006.

Xia, H., Luo, H., Shan, C., Muruato, A.E., Nunes, B.T.D., Medeiros, D.B.A., Zou, J., Xie, X., Giraldo, M.I., Vasconcelos, P.F.C., Weaver, S.C., Wang, T., Rajsbaum, R., Shi, P.Y., 2018. An evolutionary NS1 mutation enhances Zika virus evasion of host interferon induction. Nat. Commun. 9, 414.

Xiang, W., Zhang, Q., Lin, X., Wu, S., Zhou, Y., Meng, F., Fan, Y., Shen, T., Xiao, M., Xia, Z., Zou, J., Feng, X.H., Xu, P., 2016. PPM1A silences cytosolic RNA sensing and antiviral defense through direct dephosphorylation of MAVS and TBK1. Sci. Adv. 2,

e1501889.
Yang, L., Wang, R., Yang, S., Ma, Z., Lin, S., Nan, Y., Li, Q., Tang, Q., Zhang, Y.J., 2018. Karyopherin alpha 6 is required for replication of porcine reproductive and respiratory syndrome virus and zika virus. J. Virol. 92 (pii: e00072-18).
Yin, X., Li, X., Ambardekar, C., Hu, Z., Lhomme, S., Feng, Z., 2017. Hepatitis E virus persists in the presence of a type III interferon response. PLoS Pathog. 13, e1006417.
Zhao, B., Yi, G., Du, F., Chuang, Y.C., Vaughan, R.C., Sankaran, B., Kao, C.C., Li, P., 2017. Structure and function of the Zika virus full-length NS5 protein. Nat. Commun. 8, 14762.